A&A 434, 887–894 (2005)
DOI: 10.1051/0004-6361:20041401

Astronomy & Astrophysics

HI-observations of blue compact dwarf galaxies⋆

W. K. Huchtmeier[1], G. Krishna[2], and A. Petrosian[3]

[1] Max-Planck-Institut für Radioastronomie, Auf dem Hügel 69, 53121 Bonn, Germany
e-mail: huchtmeier@mpifr-bonn.mpg.de
[2] NCRA-TIFR, Pune University Campus, Pune – 411 007, India
e-mail: krishna@ncra.tifr.res.in
[3] Byurakan Astrophysical Observatory and Isaac Newton Institute of Chile, Armenian Branch, Byurakan – 378433, Armenia
e-mail: artptrs@yahoo.com

Received 3 June 2004 / Accepted 7 January 2005

Abstract. We present HI-observations of 56 blue compact dwarf (BCD) galaxies of which 44 have been detected in the 21-cm line from neutral hydrogen with the 100-m radiotelescope at Effelsberg. Optical data (e.g., from NED) and HI data from other observers and telescopes are used to estimate the likelihood of confusion from other galaxies within the Effelsberg beam. The selected 29 BCD galaxies without any sign of confusion are used to infer several characteristic properties of the BCD galaxy population. In some respects, they resemble normal galaxies: e.g., the relations between global parameters like linear diameter A_0 versus blue luminosity L_B and the $M_{\rm HI}/L_B$ ratio vs. L_B. At least five of these BCDGs emit milli-Jansky level radio continuum emission.

Key words. galaxies: dwarf – galaxies: evolution – galaxies: fundamental parameters

1. Introduction

A small but remarkable minority of nearby dwarf galaxies, called Blue Compact Dwarf Galaxies (BCDG), are characterized by not just a low intrinsic luminosity ($M_B \geq -17$) and a barely resolved appearence on the Palomar-Sky-Survey plates, but also a blue color, low metallicity (∼10% solar) and sharp narrow emission lines superposed on a blue continuum (Sandage & Binggeli 1984; Thuan 1991). On high-resolution images BCDGs appear as a small group of emission knots (star-forming 30 Doradus type) often distributed around the center of an underlying faint fuzz resembling an irregular galaxy (e.g. Thuan et al. 1997). Due to the low metallicity and the considerable gas consumption involved in the violent star formation, it is mostly believed that unlike spirals, the star formation in BCDGs takes place in transient, sporadic bursts within either an already evolved galaxy or, possibly, in some cases like I Zw 18, in a relatively young galaxy (Kunth & Sargent 1986; Thuan 1991; Legrand et al. 2000). Such gas-rich, metal-poor dwarfs offer a rare opportunity to view galaxy formation from close proximity (Kunth & Östlin 2000). Moreover, BCDGs may also provide a link to the enigmatic "blue dwarf" population that dominates the faint galaxy counts. As recently as $z = 0.3$ to 0.5, such galaxies were an order-of-magnitude more populous than normal bright galaxies and yet curiously, they have faded to obscurity by $z \sim 0.1$ (e.g. Babul & Rees 1992). Many observational studies of BCDGs have been carried out in different wavelengths for different samples of these galaxies. Particularly, several studies have been done to examine neutral hydrogen content and its structure in BCDGs (e.g. Lequeux & Viallefond 1980; Thuan & Martin 1981; Viallefond & Thuan 1983; Thuan et al. 1999a; Comte et al. 1999; Pustilnik et al. 2002), which are crucial for the understanding of the nature and evolution of these objects. In this paper we present a set of HI observations for a sample of BCDGs assembled from the First and Second Byurakan objective prism surveys. The sample of BCDGs is presented in Sect. 2. We discuss the HI observations in Sect. 3. In Sect. 4 we describe observed HI data and present observed HI profiles. Section 5 presents main results for our sample galaxies as well as comments on individual galaxies. Discussion (Sect. 6) finalizes the paper.

2. The sample of BCDGs

The sample of BCDGs has been selected from the First and Second objective prism surveys of active and star forming galaxies conducted at Byurakan Observatory (Armenia):

– the First Byurakan Survey (FBS) or Markarian survey (Markarian 1967 and following papers), on which complete information is given by Mazzarella & Balzano (1986), Markarian et al. (1989) and Petrosian et al. (2004a);

⋆ Tables 1 and 2 are only available in electronic form at the CDS via anonymous ftp to cdsarc.u-strasbg.fr (130.79.128.5) or via http://cdsweb.u-strasbg.fr/cgi-bin/qcat?J/A+A/434/887

– the Second Byurakan Survey (SBS) (Markarian & Stepanian 1983, and following papers), on which complete information is presented by Bicay et al. (2000) and Petrosian et al. (2004b).

The selection criteria for the BCDGs sample are:

– $M_{\rm p}$ approximately fainter than −17 m for H_0 = 75 km s^{-1} Mpc^{-1};
– compact structure. Clear absence of spiral arms or obvious irregular morphology confirmed by high resolution imaging;
– the existence of strong, and narrow emission lines.

3. H I-observations

Observations were performed using the 100-m radiotelescope at Effelsberg which has a half power beam width of 9.3′ at a wavelength of 21 cm. The 1024-channel autocorrelator was split into four filter banks (256 channels each) using a bandwidth of 6.25 MHz which yielded a resolution of 6 km s^{-1} or 10 km s^{-1} after Hanning smoothing. A typical observing time of 60 min per source yielded a rms noise of ∼4 mJy (the system noise was 30 K). Most observations have been repeated in order to achieve a higher signal-to-noise ratio. An ON-source position was combined with an OFF-source position every 5 min. This total power mode improves the baseline behavior of the spectra. Regular measurements of well known continuum sources were used to control pointing and calibration of the telescope. Every two to three hours a well known line source (e.g. dwarf galaxies) was used as a system check. The *toolbox* software of the MPIfR was used for the data reduction. The observed spectra were corrected for moderately curved baselines only; this should not introduce additional errors in the estimated velocities and flux densities of the lines since the line profiles are quite narrow in all cases.

4. The basic results

The HI profiles for the 44 detected galaxies are shown in Fig. 1. 21 of these galaxies have been observed for the first time. Table 1 gives the corresponding HI flux in [Jy km s^{-1}] and the heliocentric radial velocities in km s^{-1}. The narrow profiles in Fig. 1 correspond to dwarfish galaxies (i.e. $M^{0,i}_{B,T}$ fainter than −15). In some profiles we have cut out the local HI emission from our galaxy (in fact the difference of the local emission between the ON and OFF positions – total power mode) as it was much stronger than the extragalactic emission.

In Table 1 we present the observational data: the galaxy name in Col. 1; coordinates (J2000) used for the observations, more precise optical coordinates will be published by Petrosian et al. (2004a,b); the morphological type in Col. 3, where "Int" means interacting galaxies; the optical dimensions in arcsec corresponding to the blue surface brightness level at 25 mag arcsec^{-2} in Col. 4; the total blue apparent magnitude in Col. 5 (HYPERLEDA[1]); for SBS1331+493 and SBS1428+457 from Doublier et al. (1997); the optical heliocenctric radial velocity in Col. 6. The HI data follow, i.e., the measured HI flux (Col. 7), the observed peak flux of the line and its rms error in Col. 8 (for non detections only the rms noise is shown), the heliocentric radial velocity derived from the midpoint of the line at 50% of the peak and its error (Col. 9), and the linewidth at a level of 50% of the line peak and, whenever clearly above the noise, the 20% level (Col. 10).

The derived global parameters for our sample of galaxies are presented in Table 2, the galaxy name (SBS if not otherwise stated) in Col. 1, the optical heliocentric velocity (Table 1, Col. 6) has been reduced to the frame of the cosmic microwave background (using NED) $V_{3K\rm bgd}$ (Col. 2). We did not use the more accurate HI velocities because of possible confusion in some cases. The distances in Col. 3 have been derived taking a Hubble constant $H_0 = 72$ km s^{-1} Mpc^{-1} (Freedman et al. 2001). Optical diameters in the D_{25} system (Table 1, Col. 4) have been corrected for absorption and for inclination, where the inclination was derived from the axial ratio assuming an intrinsic axial ratio of 0.2 (e.g. Tully 1985, in view of the uncertainties in these inclinations we did not apply corrections for possible type dependance of the intrinsic axial ratio):

$$\log a_0 = \log\ a + 0.09\,A_b - 0.2\,\log(a/b),$$

where the foreground absorption in the blue A_b is from Schlegel et al. (1998) (as given in the NED).

The linear diameter $A_{0,i}$ [kpc] follows in Col. 4, the absolute magnitude $M^{0,i}_{b,t}$ corrected for Galactic extinction (Schlegel et al. 1998) and internal absorption in Col. 5. The internal absorption in a galaxy in the B-band, A_i, depends on inclination and luminosity (Giovanelli et al. 1994; Tully et al. 1998; Verheijen 2001; Karachentsev et al. 1999):

$$A_i = [1.6 + 2.8(\log V_m - 2.2)] \times \log(a/b);\ V_m \geq 42.7 \text{ km s}^{-1}$$

$$A_i = 0 - \text{other}$$

$$A_i = 0 - \text{E, S0, dSph.}$$

Here we use the following definition of V_m: the HI rotational velocity $V_m = W_{50}/(2\sin i)$ corrected for inclination and turbulent motion (Tully & Fouqué 1985) with isotropic non-circular motion parameter $\sigma_z = 8$ km s^{-1}.

The total H I mass (Col. 6) has been calculated using

$$M_{\rm H\,I} = 2.355 \times 10^5\, D^2 \int S_v {\rm d}v,$$

where D is the distance in Mpc and $\int S_v {\rm d}v$ is the integrated HI-flux in Jy km s^{-1}.

The total mass $M_{\rm T}$ (Col. 7) has been derived by

$$M_{\rm T} = \text{const.}\, D\, a_0\, \Delta\, v^2_{0,i},$$

where D is the distance in Mpc, a_0 the corrected optical diameter in arcmin, const. = 33 110, and $\Delta\ v_{0,i}$ the corrected edge-on linewidths at 50% of the peak flux (e.g. Karachentsev et al. 2004).

[1] http://www-obs.univ-lyon1.fr/hypercat/

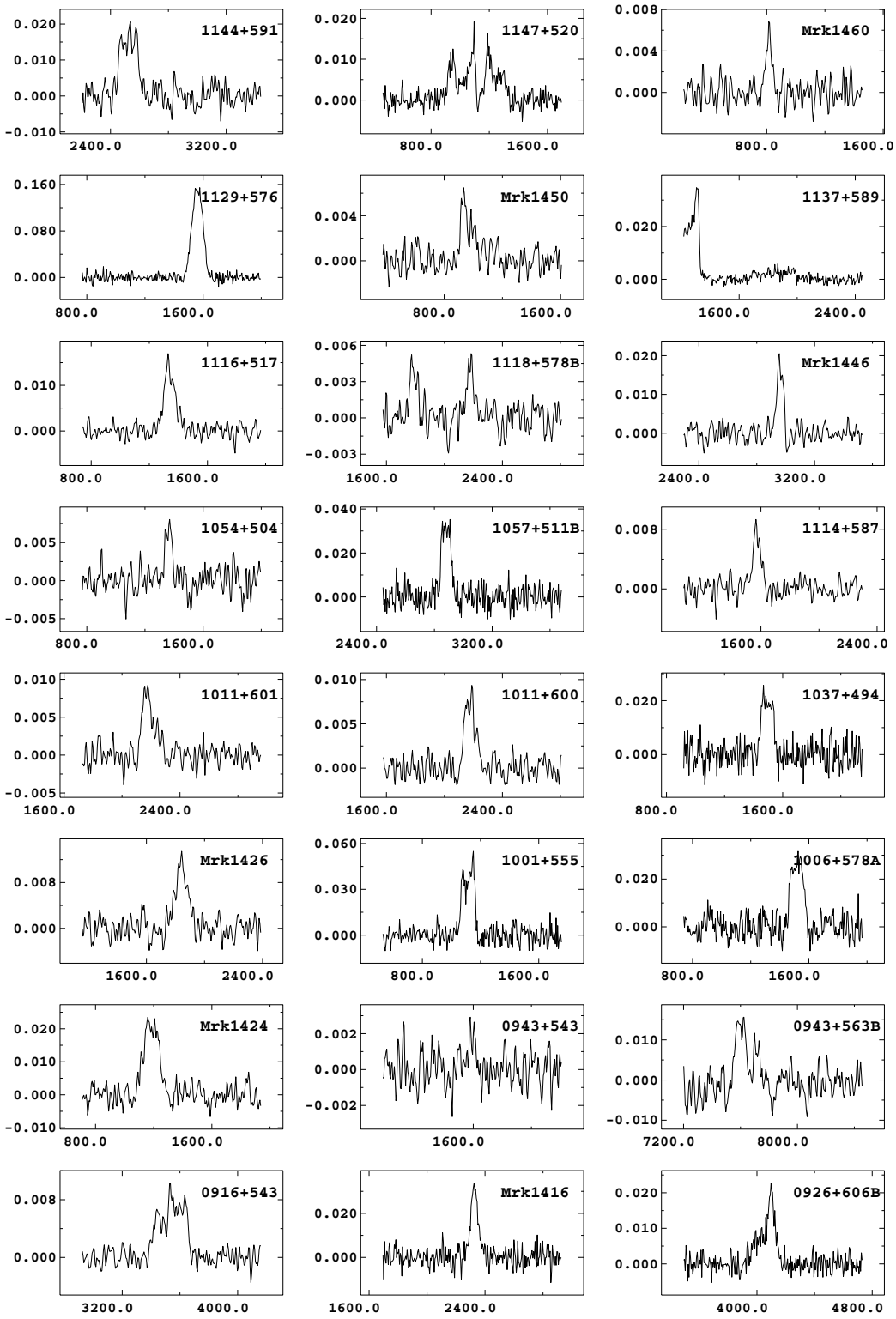

Fig. 1. HI profiles of the 44 detected galaxies observed with the 100-m Effelsberg radio telescope which has a half power beamwidth of 9.3 arcmin at 21-cm. 21 of theses galaxies have been observed for the first time. Profiles are arranged in increasing order of right ascension, starting at the bottom left of this figure (see Table 1). The axes are given in Jansky (Jy) and in heliocentric radial velocity in km s^{-1}.

The HI mass-to-luminosity ratio $M_{\rm HI}/L_B$, the mass-to-luminosity ratio $M_{\rm T}/L_B$, and the relative HI mass $M_{\rm HI}/M_{\rm T}$ follow in Cols. 8 to 10, respectively. A "c" in Col. 11 indicates that the HI data are (probably) confused by neighboring galaxies within the antenna beam (Sect. 4). Many galaxies in our sample have been observed for HI emission using the Nançay radio telescope, with a half power beamwidth of $3.7' \times 22'/\cos$ (declination) in RA and dec respectively, Thuan et al. (1999a, TLMP hereafter). In Sect. 4 we include comments on those data, keeping in mind that the confusion expected

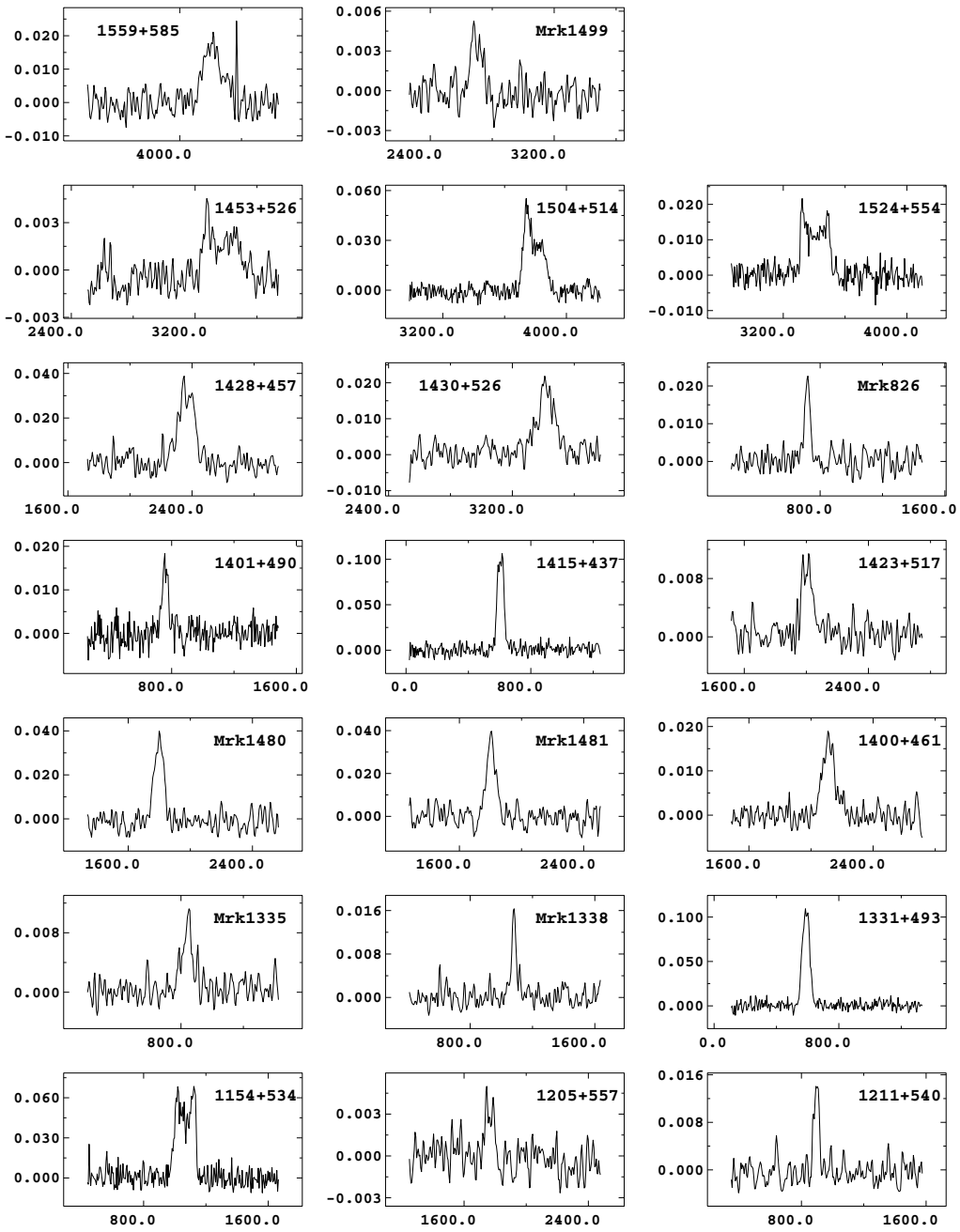

Fig. 1. continued.

from other galaxies within their beam can be quite different from that present in our observations, due to the very different beam shapes. Also, in most cases, the present observations achieved a higher sensitivity.

The radio continuum parameters of the detected BCDGs are based on the NVSS[2] and/or the FIRST[3] surveys at 1.4 GHz (Sect. 4).

5. Comments on individual galaxies

SBS 0916+543 – confused area (POSS), several galaxies within 5 arcmin (NED); optical velocities known for two galaxies: SBS 0916+543 (3582 ± 18 km s^{-1}) and another elongated galaxy of similar brightness (2.6 arcmin SW at 3640 ± 46 km s^{-1}); the Nançay HI profile (TLMP) shows a narrow line (of 0.75 ± 0.2 Jy km s^{-1}) peaked at the optical radial velocity of the target galaxy. The large difference in line shape and flux between the Effelsberg and Nançay profiles can be understood in terms of several confusing galaxies seen with the different beam shapes. Only the central peak seen in our spectrum is clearly detected in the Nançay observation.

Mrk 1416 – HI profiles from Nançay (1.96 ± 0.32 Jy km s^{-1}, TLMP) and Effelsberg are consistent. No obvious sign of confusion. Large color variations are seen in the optical images (Doublier et al. 1997).

[2] NRAO VLA Sky Survey at 20 cm, Condon et al. (1998).
[3] Faint Images of the Radio Sky at 20 cm, Becker et al. (1995).

SBS 0926+606 B – confused by SBS0926+606A (1.5 arcmin south, optical velocity v = 4002 km s^{-1}). The higher velocity peak of the HI profile agrees in velocity with galaxy B (v = 4150 km s^{-1}) and the low velocity extension matches with galaxy A.

Mrk 1424 – HI profiles from Effelsberg and Nançay (2.46 ± 0.37 Jy km s^{-1}, TLMP) are consistent.

SBS 0943+563 – Two adjacent narrow HI profiles? Possible interaction with a 15.2 m_{pg} galaxy (Mrk 0123, v = 7630 km s^{-1}) at 0.5 arcmin.

Mrk 1426, SBS 0946+487 – Centrally peaked HI profile with wide wings. Profile shape is atypical for an undisturbed galaxy, possible confusion from nearby galaxies.

SBS 1001+555, UGC 05421 – HI data from Effelsberg are consistent with data from Green Bank (Schneider et al. 1992; Haynes & Giovanelli 1991; Theureau et al. 1998, TLMP).

SBS 1006+578 – HI data from Effelsberg and Nançay (TLMP) are consistent.

SBS 1011+601 – SBS 1011+601 (v = 2160 km s^{-1}), SBS 1011+600 (v = 2188 km s^{-1}) 2.2 arcmin south: possible confusion. The small spatial separation of 2.2′ and the small velocity separation makes it impossible to separate the HI contribution from each of these galaxies. The asymmetric high velocity wing – seen in both Effelsberg profiles – is too faint to stand out in the published Nançay (0.52 ± 0.19 Jy km s^{-1}, TLMP) profile.

SBS 1011+600 – Interacting pair with SBS 1011+601 (2.2 arcmin north, see above).

Mrk 1434 – Our deeper observation improves the HI upper limit from Nançay (TLMP) by a factor of 1.7. Optical observations show a bright central component and a de Vaucouleurs profile (Doublier et al. 1997).

SBS 1037+494 – The noisy Nançay (TLMP) profile does not show structural details but generally (radial velocity, flux) agrees with our observation.

SBS 1054+504 – Our data puts on a fine footing the marginal Nançay (0.58 ± 0.21 Jy km s^{-1}, TLMP) detection of the galaxy. Elliptical like galaxy with a de Vaucouleurs profile, a color gradient and a redder outer envelope (Doublier et al. 1997).

SBS 1057+511B – SBS 1057+511B (v = 3055 km s^{-1}) is located 3.5 arcmin south of UGC 6074 (v = 2890 km s^{-1}). SBS 1057+511B is a giant HII region or projected BCG in/on MCG+09-18-067 (Petrosian et al. 2002). UGC 6074 is clearly detected in the Green Bank observation. Our profile agrees well in velocity and line width with the Green Bank profile (as well as with the optical velocity of UGC 6074 (v = 2889 ± 14 km s^{-1}). The offset of our beam centre from UGC 6074 (3.5 arcmin) can account for our detecting only about 50% of the flux measured at Green Bank. Therefore, our HI profile probably corresponds to UGC 6074.

SBS 1114+587 – Our observation with improved sensitivity confirms the Nançay detection (TLMP) but instead reveals a distinctly more narrow profile.

SBS 1116+517 – Arp's galaxy; SBS 1116+518, v = 30 879 km s^{-1} (NED) located 3 arcmin north.

SBS 1118+578B – SBS 1118+578A (v = 2163 km s^{-1}) at 2 arcmin NW, pair of galaxies. Our profile shows two clear peaks at v = 2176 ± 20 km s^{-1} and at v = 1791 ± 11 km s^{-1}. The galaxy counterpart for the other peak is unclear.

Mrk 1446 – Good agreement between Effelsberg and Nançay (0.99 ± 0.2 Jy km s^{-1}, TLMP) observations for the radial velocity and the HI-flux. We find a much narrower line (W_{50} = 50 km s^{-1}) due to our higher sensitivity.

SBS 1123+576 – The marginal detection at Nançay (0.12 ± 0.08 Jy km s^{-1}, TLMP) is not confirmed in our observations.

SBS1129+576 – Likely confusion with irregular type galaxy MCG+10-17-10 (v = 1457 km s^{-1}, NED) 1.3^s E, 3.8′ N (projected separation of 20 kpc). Green Bank observation (21.62 ± 0.8 Jy km s^{-1}) agree in radial velocity and line width at the 50% level with the Effelsberg data.

Mrk 1450 – Effelsberg data show a clear 6 sigma detection (with a rms noise of 1 mJy), the Nançay data yield an rms noise of 2.8 mJy (TLMP).

SBS 1137+589 – NGC 3795 (v = 1210 km s^{-1}) located 3.7′ away (part of the HI emission due to this galaxy is seen at the low velocity end of the presented profile, Fig. 1), causes no confusion because of the different radial velocities. The faint wide emission in the center of the profile is unlikly due to the SBS galaxy only (e.g. SBS 1137+588, v = 2310 km s^{-1}, is within the beam).

SBS 1144+591 – Nearby galaxies in the beam, without velocity information. The Nançay profile is highly asymmetric in contrast to our HI profile. The two agree in linewidth W_{20} but not in W_{50} (84 vs. 137 km s^{-1}). The difference in line shape and width between the Effelsberg and the Nançay (TLMP) profiles could be due to different confusion within the two telescope beams. The NVSS map shows a resolved radio source of ∼1 arcmin extent with a flux of ∼6 ± 2 mJy at 1.4 GHz. The radio peak at 11h 47m 17.7s, +58° 53′ 40″ (J2000) is offset from the BCDG position by ∼0.5′ to NW.

SBS 1147+520 – This HI profile is heavily confused by two bright galaxies, UGC 6802 (7′ N) and NGC 3917 (9.5′ NE). SBS 1147+520 (v = 1257 km s^{-1}) is confused with UGC 6802 (v = 1253 km s^{-1}, the integrated HI profile extends from 1180 to 1300 km s^{-1}), while the integrated HI profile of NGC 3917 (v = 965 km s^{-1}) extends from 830 to 1120 km s^{-1}. The Nançay (TLMP) and Effelsberg profiles differ markedly both in line shape and width. The narrow (EW) but highly elongated (NS) Nançay beam might be sensitive to UGC 6802 (7′N). Our profile consists of three main components at velocities 949, 1077, and 1224 km s^{-1}. The first two peaks are not at all detected in the Nançay profile which shows a clear peak around 1200 km s^{-1}, comparable to our third peak. Further, they detect stronger emission around 1300 km s^{-1}, which is barely seen in our profile. Our first peak (v = 949 km s^{-1}) matches in velocity with NGC 3917 (9.5′ NE); this could not be seen with the Nançay beam due to its different shape and size. Our second peak (v = 1077 km s^{-1}) is not seen in the Nançay

profile. It could be associated with the present SBS galaxy (optical radial velocity is close). Our third HI component could be identified as the attenuated peak due to UGC 6802, which is seen at a stronger level in the Nançay observations (Thuan et al. 1999b, TLMP), due to their highly elongated NS beam.

Mrk 1460 – Very faint galaxy with a narrow HI line.

SBS 1154+534 – UGC 6923. Double horn HI profile of a late type galaxy, consistent with Nançay observation (Comte et al. 1999). The NVSS image shows a radio counterpart of 7.3 ± 2.1 mJy at 1.4 GHz, with an overall extent of ∼2′ in the NS direction. The structure is very diffuse, as it is not detected in the FIRST image (hence, any sub-arcsecond scale emission must be below 0.5 mJy at 1.4 GHz).

SBS 1205+557 – General agreement with the marginal Nançay profile (TLMP).

SBS 1211+540 – Excellent agreement with the Nançay profile (0.71 ± 0.12 Jy km s^{-1}, TLMP).

HI radial velocity agrees with the marginal detection at Nançay (Comte et al. 1999).

SBS 1331+493 – Excellent agreement with Nançay profiles (TLMP).

Mrk 1480, Mrk 1481 – Mrk 1481 at 1.7′, possible confusion. Our profiles of this pair of galaxies (separation 1.7 arcmin), pointed at each of them, have very similar parameters. The angular resolution is totally inadequate to separate the contributions of the individual galaxies. Good agreement with Nançay profile (TLMP).

SBS 1400+461 – Agreement with Nançay data (TLMP). NVSS image shows a marginally detected radio counterpart with 3.2 ± 1.0 mJy at 1.4 GHz. No detection in the FIRST survey, however.

SBS 1401+490 – Good agreement with Nançay profile (TLMP). A galaxy of comparable brightness is seen 2.1′ NW (v = 25 360 km s^{-1}, NED).

SBS 1413+495A – Detected at Nançay (TLMP), with 1.18 Jy km s^{-1}. A bright galaxy nearby (2.5′ SE, v = 7951 km s^{-1}).

SBS 1415+437 – Excellent agreement with Nançay data (4.73 ± 0.32 Jy km s^{-1}, Comte et al. 1999). NVSS image shows an unresolved radio counterpart of 2.0 ± 0.5 mJy at 1.4 GHz. No detection in the FIRST survey, hence no arcsec-scale structure above 0.5 mJy limit at 1.4 GHz.

SBS1423+517 Clear detection of a well resolved HI line (W_{50} = 79 km s^{-1}). Undetected at Green Bank (TLMP) because of higher noise (rms = 7.6 mJy).

SBS 1428+457 – Good agreement with Nançay observation (Comte et al. 1999). Bright star forming region in the center, multiple knots (Doublier et al. 1997).

SBS 1430+526 – HI profile at v = 3420 km s^{-1} is in good agreement with Nançay data (TLMP). Some contribution is possible from a slightly brighter galaxy (5.5′ NW). The optical velocity of SBS 1430+526 is v = 3180 km s^{-1} (Petrosian et al. 2002).

Mrk 475 – Not detected in Effelsberg. The Nançay detection of 0.15 ± 0.04 Jy km s^{-1} (TLMP) would correspond to a three σ signal at our sensitivity.

Mrk 826 – The narrow HI feature in our spectrum agrees with the weakly detected feature in the Green Bank spectrum (1.09 ± 0.5 Jy km s^{-1}, TLMP).

SBS 1453+526 – Optical velocity is $v_{\rm opt}$ = 3280 km s^{-1} (TLMP); no detection at Green Bank (rms noise 7.5 mJy, TLMP). Broad double-horned HI profile, rules out a dwarf galaxy, despite its optical faintness (Fig. 1; Table 1).

SBS 1504+514 – Good agreement with the Nançay HI profile (TLMP). However, too bright to be a dwarf galaxy (Table 1). NVSS image shows a marginally detected radio counterpart with 1.5 ± 0.5 mJy at 1.4 GHz. The clear double horn profile signifies a rotating HI disk.

SBS 1524+554 – Excellent agreement with the Nançay profile (2.43 ± 0.21 Jy km s^{-1}, TLMP).

SBS 1555+515 – Optical and HI velocities (TLMP) differ by 200 km s^{-1}. Hence we treat this galaxy as non-detected in HI. Thuan et al. (1999b) suggest the possibility of confusion from a galaxy 1.1s E and 7′ N (unknown velocity). If the wide HI profile seen by (TLMP) would be associated with this Sc galaxy, we would not be able to detect it (due to our much narrower beam in that direction).

SBS 1559+585 – A two magnitude fainter galaxy SBS 1558+585 (v = 4218 ± 13 km s^{-1}) is located 2.2′ W. The unusual shape of the HI profile suggests that we are seeing emission from both galaxies, which is supported by the higher HI flux measured with the Effelsberg beam. NVSS image shows a radio counterpart with 3.6 ± 0.9 mJy at 1.4 GHz, extended NS by ∼1′. Its non-detection in the FIRST survey means that it has no arcsecond-scale emission above 0.5 mJy at 1.4 GHz.

Mrk 1499, UGCA 412 – Good agreement with the Nançay observation (0.44 ± 0.11 Jy km s^{-1}, TLMP). Bright elongated very blue central structure with two components (Doublier et al. 1997). The object is detected at 1.4 GHz in both NVSS and FIRST surveys. The NVSS image is confused by a (probably unrelated) double radio source, which causes a large uncertainty in the derived parameters. We estimate for the BCDG a flux of 2.5 ± 1 mJy at 1.4 GHz, out of which ∼1 mJy is contained within the 5″ beam of the FIRST survey.

SBS 1723+565 – Several galaxies with similar radial velocities within the antenna beam; no HI detection, however. From a comparison of the NVSS and FIRST images, we identify this BCDG with a radio source of 5.8 ± 0.9 mJy at 1.4 GHz, out of which 3.1 ± 0.3 mJy lies within a ≤5″ component at RA (J2000) = 17h 24m 38.00s, Dec = +56°28′37.6″. The remaining flux comes from a larger component extended by ∼1′.

As seen from the above comments, the availability of HI observations from other radio telescopes, differing in beam sizes and shapes, has often been very useful in estimating/resolving possible confusion arising from nearby galaxies. Based on this discussion we have been able to identify those galaxies in our sample, for which our HI observations are likely

Table 3. The derived global characteristics of BCDGs compared with the Salzer et al. (2002) sample.

	BCDG sample			Salzer sample		
	median	min	max	median	min	max
A_0 [kpc]	3.1	1.0	7.5	3.2	0.5	11
M_B	–15.5	–12.4	–17.4	–16.1	–12	–17.5
$M_{\rm HI}$ [10^8 $M_\odot$]	1.5	0.9	14.5	3.0	0.2	18
W_{50} [km s^{-1}]	58	29	190	88	30	220

to be significantly confused. These objects are marked with a "c" (for confused) in the last column of Table 2.

6. Discussion

We will not consider the two galaxies brighter than $M_B = -18$ as they do not satisfy the magnitude criterion adopted for BCDGs in Sect. 2. Additional 4 objects are slightly brighter than $M_B = -17$ which was the approximate brightness limit given in Sect. 1 for BCDGs. Out of these brighter objects only one has been classified as a pure BCD galaxy (Mrk 1499), the others are of type S0, Sc, or BCD/Im. The median of the distribution of the absolute magnitude is $M_B = -15.1$ with the weakest object at $M_B = -12.4$. The median of the linear optical diameter corresponding to the D_{25} system (de Vaucouleurs et al. 1976) is 2.7 kpc, extreme values are 10 kpc and 0.5 kpc.

The HI profiles of the brighter galaxies in our sample (around $M_B = -17$) have greater line widths (~100 km s^{-1}) and show the typical double-horn structure signifying rotating HI disks. Narrow single-peaked HI lines (≤50 km s^{-1}) are typical for the weakest and smallest galaxies in our sample.

For the characterization of the HI and related parameters of BCDGs we henceforth use only the 29 galaxies (fainter than $M_B = -18$) with no indications of confusion. The median values of range spanned by the global parameters for these 29 galaxies are given in Table 3 together with the values of a sample of 122 actively star-forming galaxies (Salzer et al. 2002). They describe the population of dwarfish HI-rich galaxies. The global parameter or ratio is given in Col. 1, the median value of the parameter in Col. 2, the maximum and minimum values of the parameter in Cols. 3 and 4, the corresponding values from the comparison sample (Salzer et al. 2002) follow in Cols. 5 to 7. The general agreement in global parameters for these two samples of galaxies suggests that we deal with similar galaxies in both samples. However, the Salzer et al. (2002) sample contains objects with different morphological structure and different levels of activity.

The dependence of the distance-independent ratio $M_{\rm HI}/L_B$ on absolute blue magnitude (Fig. 2) is also similar to that found for other comparison samples; e.g. the catalog of nearby galaxies (distance ≤ 10 Mpc, Karachentsev et al. 2004, hereafter KKHM).

The Holmberg relation (linear diameter A_0 versus absolute blue magnitude: Fig. 3) for this sample of BCDGs is found to be similar to samples of normal galaxies. In both Figs. 2 and 3 the straight line shows the correlation found for the comparison sample (KKHM) over the whole range of M_B covered by it. The good agreement between the correlations between the global parameters for BCDGs and the normal galaxies appears to suggest that, at least in a statistical sense, the influence of the starbursts in BCDGs is relatively localized and does not disrupt the evolution of the galaxy on a global scale.

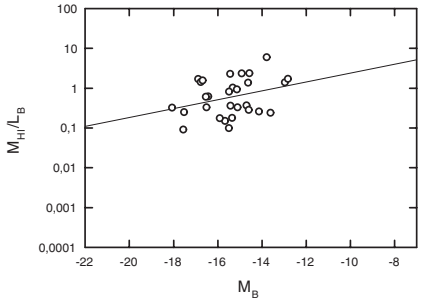

Fig. 2. The relative content of neutral hydrogen $M_{\rm HI}/L_B$ of the detected galaxies is plotted versus blue absolute magnitude M_B. The solid line represents the sample of nearby galaxies (KKHM). The range covered by both coordinates is the total range covered by the comparison sample.

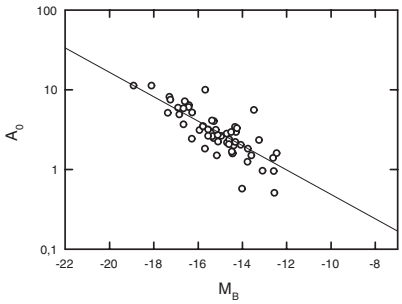

Fig. 3. The linear diameter A_0 is given versus the absolute blue magnitude of all galaxies of our sample. The solid line represents the sample of nearby galaxies (KKHM). The range covered by both coordinates is the total range covered by the comparison sample.

Acknowledgements. Based on observations with the 100-m radio telescope of the MPIfR (Max-Planck-Institut für Radioastronomie) at Effelsberg. We have made extensive use of the NASA/IPAC Extragalactic Database (NED, which is operated by the Jet Propulsion Laboratory, Caltech, under contract with the National Aeronautics and Space Administration), and the Digitized Sky Survey (DSS–1) produced at the Space Telescope Science Institute under US Goverment grant NAG W–2166. G.K. thanks the Alexander von Humboldt-Foundation for a Senior Research Fellowship.

References

Babul, A., & Rees, M. J. 1992, MNRAS, 255, 346

Becker, R. H., White, R. L., & Delfand, D. J. 1995, ApJ, 450, 559 (FIRST)

Bicay, M. D., Stepanian, J. A., Chavushyan, V. H., et al. 2000, A&AS, 147, 169

Comte, G., Petrosian, A. R., Ohanian, G. A., & Stepanian, J. A. 1999, Astrophys., 42, 149

Condon, J. J., Cotton, W. D., Greisen, E. W., et al. 1998, AJ, 115, 1693 (NVSS)

de Vaucouleurs, G., de Vaucouleurs, A., & Corwin, H. G., Jr. 1976, Second Reference Catalogue of Bright Galaxies (Austin: Univ. of Texas Press) (RC2)
Doublier, V., Comte, G., Petrosian, A., Surace, C., & Turatto, M. 1997, A&AS, 124, 405
Freedman, W. L., Madore, B. F., Gibson, B. K., et al. 2001, ApJ, 553, 47
Giovanelli, R., Haynes, M. P., Salzer, J. J., et al. 1994, AJ, 107, 2036
Haynes, M. P., & Giovanelli, R. 1991, ApJS, 77, 331
Karachentsev, I. D., Makarov, D. I., & Huchtmeier, W. K. 1999, A&AS, 139, 97
Karachentsev, I. D., Karachentseva, V. E., Huchtmeier, W. K., & Makarov, D. I. 2004, AJ, 127, 2031 (KKHM)
Kunth, D., & Östlin, G. 2000, A&ARv, 10, 1
Kunth, D., & Sargent, W. L. W. 1986, ApJ, 300, 496
Legrand, F. 2000, A&A, 354, 504
Legrand, F., Kunth, D., Roy, J.-R., Mas-Hesse, J. M., & Walsh, J. R. 2000, A&A, 355, 891
Lequeux, J., & Viallefond, F. 1980, A&A, 91, 269
Markarian, B. E. 1967, Astrophys., 3, 34
Markarian, B. E., & Stepanian, J. A. 1983, Astrophys., 19, 354
Markarian, B. E., Lipovetskii, V. A., Stepanian, J. A., Erastova, L. K., & Shapovalova, A. I. 1989, Soobshch. Spets. Astrofiz. Obs., 62, 5
Mazzarella, J. M., & Balzano, V. A. 1986, ApJS, 62, 751
Petrosian, A., McLean, B., Allen, R. J., et al. 2002, AJ, 123, 2280
Petrosian, A. R., McLean, B., Allen, R. J., & MacKenty, J. 2004a, in preparation
Petrosian, A. R., McLean, B., Stepanian, J. A., et al. 2004b, in preparation
Pustilnik, S. A., Martin, J.-M., Huchtmeier, W. K., et al. 2002, A&A, 389, 405
Salzer, J. J., Rosenberg, J. L., Weisstein, E. W., Mazzarella, J. M., & Bothun, G. D. 2002, AJ, 124, 191
Sandage, A., & Binggeli, B. 1984, AJ, 89, 919
Schlegel, D. J., Finkbeiner, D. P., & Davies, M. 1998, ApJ, 500, 525
Schneider, S. E., Thuan, T. X., Mangum, J. G., & Miller, J. 1992, ApJS, 81, 5
Theureau, G., Bottinelli, L., Coudreau-Durand, N., et al. 1998, A&AS, 130, 333
Thuan, T. X. 1991, in Massive stars in starbursts, ed. C. Leitherer, N. R. Walborn, T. M. Heckman, & C. A. Norman (Cambridge: Cambridge University Press), 183
Thuan, T. X., & Martin, G. E. 1981, ApJ, 247, 823
Thuan, T. X., Isotov, Y. I., & Lipovetsky, V. A. 1997, ApJ, 477, 661
Thuan, T. X., Lipovetsky, D. A., Martin, J.-M., & Pustilnik, S. A. 1999a, A&AS, 139, 1 (TLMP)
Thuan, T. X., Isotov, Y. I., & Foltz, C. B. 1999b, ApJ, 525, 105
Thuan, T. X., Hibbard, J. E., & Lèvrier, F. 2004, AJ, 128, 617
Tully, R. B. 1985, Nearby Galaxies Catalog (Cambridge: Cambridge University Press)
Tully, R. B., & Fouqué, P. 1985 ApJS, 58, 67
Tully, R. B., Pierce, J., Huang, J. S., et al. 1998, AJ, 115, 2264
Verheijen, M. A. W. 2001, ApJ, 563, 694
Viallefond, F., & Thuan, T. X. 1983, ApJ, 269, 444